Unwinding of the antiferroelectric helix in an electric field

P. V. Dolganov and V. M. Zhilin
Institute of Solid State Physics, Russian Academy of Sciences, 142432 Chernogolovka, Moscow District, Russia
(Received 31 January 2010; published 10 May 2010)

Using the discrete phenomenological model with interlayer anticlinic and chiral interaction, the unwinding of the antiferroelectric helix in external electric field was studied. The dependence of the helical pitch on the electric field differs essentially in antiferroelectric and ferroelectric phases. It was found that in antiferroelectric the critical electric field E_h of the transition into the unwound structure is proportional to the value of chiral interaction and does not depend on the anticlinic interaction between nearest layers. This behavior differs significantly from the case of ferroelectric in which E_h increases as the square of the chiral interaction and is inversely related to the synclinic interaction between layers. Peculiarities of the unwinding process and the dependence of the critical field E_h on model parameters are discussed. Based on our calculations, we propose an analytical equation for the critical unwinding field in the antiferroelectric.

DOI: 10.1103/PhysRevE.81.051704 PACS number(s): 61.30.Gd, 61.30.Cz

I. INTRODUCTION

The behavior of polar liquid crystals in external electric field is interesting both for fundamental physics and various applications. Chiral ferroelectric smectic-C^* (Sm C^*) and antiferroelectric smectic-C_A^* (Sm C_A^*) phases [1] form layer structures with long molecular axis tilted with respect to the layer normal (Fig. 1). In the Sm C^* phase the azimuthal orientation of molecules φ_i (Fig. 1) in adjacent ith and $(i+1)$th layers is nearly parallel (synclinic ordering). In the Sm C_A^* phase molecules in adjacent layers tilt in nearly opposite directions (anticlinic ordering). Layer polarization in Sm C^* and Sm C_A^* phases is perpendicular to the tilt plane. Without electric field chirality leads to rotation of the tilt plane and polarization from layer to layer and formation of a helix along the layer normal. The interaction of the electric field with layer polarization favors alignment of the tilt planes perpendicular to the electric field. The competition between chirality, which favors the helical structure, and the electric field, which favors the planar structure, leads to frustration [2]. In the electric field unwinding of the helix takes place through the formation of a complex structure with domain walls or solitons.

In nonpolar cholesteric [1] and polar Sm C^* phases unwinding of the helix in external field was investigated theoretically and experimentally in detail [3–13]. In cholesteric the molecules rotate continuously along the helical axis. In the Sm C^* phase the angle $\Delta\varphi$ between azimuthal orientations of molecules in adjacent layers is small. Without field $|\Delta\varphi|=2\pi/p_0$, where p_0 is the number of layers in the pitch. Both in cholesteric and in Sm C^* continuous theory can be used to find the equations describing the unwinding of the helix in the electric field and the value of critical field E_h of the transition to the unwound state. A more complex example of a twisted structure is the antiferroelectric helix [14] since in Sm C_A^* the molecules tilt nearly in opposite directions in nearest layers, $|\Delta\varphi|=(\pi+\alpha)$, where $\alpha=\pi/p_0$.

Muševič *et al.* used the continuous model for the description of the chiral antiferroelectric in magnetic field [15]. Their analysis of the field-induced distortion of the helical structure and the value of the critical field for unwinding of the helix were the same as in the case of chiral ferroelectric due to the similar quadratic coupling with the field. Calculations for the electric field interacting with the layer polarization were made by Taylor and co-workers [16–18]. They investigated the field-induced Fréedericksz transition and the transition to the ferroelectric structure. Then, transformation of the antiferroelectric structure in electric field was studied on a phenomenological level [19–22] and using the molecular-statistical approach [23]. In this paper, using the discrete phenomenological model [24–31] with anticlinic and chiral interaction between molecules we first calculate the variation of the antiferroelectric pitch in electric field. We found a nontrivial dependence of the critical field E_h on material parameters, which differs essentially from the dependence of E_h in the ferroelectric phase.

II. MODEL

In the antiferroelectric liquid crystal the azimuthal orientation of molecules in smectic layers can be described by a

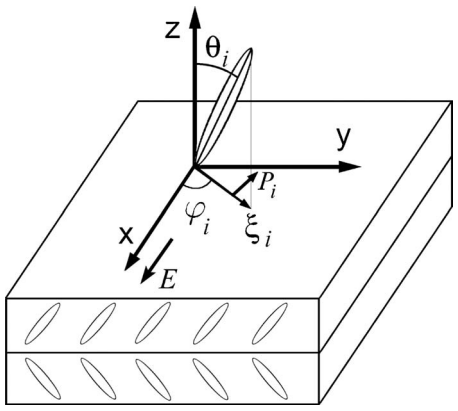

FIG. 1. Orientation of molecules and the layer structure of the tilted smectic. θ_i is the polar angle. The vector ξ_i determines the azimuthal orientation of molecules (angle φ_i). Each molecular layer bears the electric polarization P_i perpendicular to the tilt plane. The helical axis is along the layer normal. The electric field is applied along the x axis.

unit two-dimensional vector ξ_i, where the index i stands for the ith layer (Fig. 1). Using ξ_i the free energy with interaction between tilted molecules of neighboring layers can be written as

$$F = \sum_i \left[\frac{1}{2} a(\xi_i \cdot \xi_{i+1}) + f[\xi_i \times \xi_{i+1}]_z + EP_i \sin \varphi_i \right]. \quad (1)$$

Synclinic or anticlinic ordering arises due to the first term in the free energy. This interaction favors the synclinic structure for negative a and the anticlinic structure for positive a [27]. The second term (the so-called Lifshits term) describes the chiral interaction between molecules in the nearest-neighboring layers [31]. Positive or negative f corresponds to the opposite chirality. The coupling of the electric field with layer polarization P_i is described by the last term. The external electric field is parallel to the smectic layers. In our calculations the tilt angle remains constant in electric field since no intralayer interactions are considered. Antiferroelectric structures with zero-field pitch p_0 from about 40 to 80 smectic layers were calculated. These pitches correspond to selective reflection in the Sm C_A^* phase in the region from about 400 to 800 nm. In the calculations samples with periodic boundary conditions were used. The calculation of the structures in electric field was performed by means of numerical minimization of the free energy over orientation of ξ_i in all layers of the sample. The method of minimization of the free energy was described earlier [21,30]. The starting structure was taken as a random set of values of φ_i in different smectic layers. The structure with minimum energy was found by changing φ_i in every layer using the quasi-Newton algorithm. To determine the structure with the global energetic minimum, the minimizations were performed from 50 to 100 times for different random starting sets of φ_i. For the determination of the pitch p in electric field the following procedure was used. At a given E the structures with different periods were calculated. The structure with minimum energy was taken as the ground state. The calculated structures which corresponded to minimum energy were reasonable from the physical point of view, namely, helicies distorted by electric field without any defects. For the determination of E_h the structures with one soliton and without solitons were calculated in samples with periods from $3p_0$ to $6p_0$. For the structures with a soliton and without solitons calculations were performed for different values of the electric field. The electric field at which the energies of the samples with a soliton and without solitons equaled was taken as E_h. In ferroelectric structures with $|f/a| < 4 \times 10^{-2}$ the values of critical fields E_h obtained by means of the numerical calculation and from the continuous theory [1] coincided with accuracy better than 0.2%.

III. RESULTS AND DISCUSSION

The antiferroelectric and ferroelectric pitch p has been calculated using Eq. (1) as a function of the electric field E. Figure 2 shows p/p_0 in Sm C^* [Fig. 2(a)] and Sm C_A^* [Fig. 2(b)] as a function of E/E_h. The model parameters were taken to be $a=-1$ and $f=1.975\times10^{-2}$ in Sm C^* (squares),

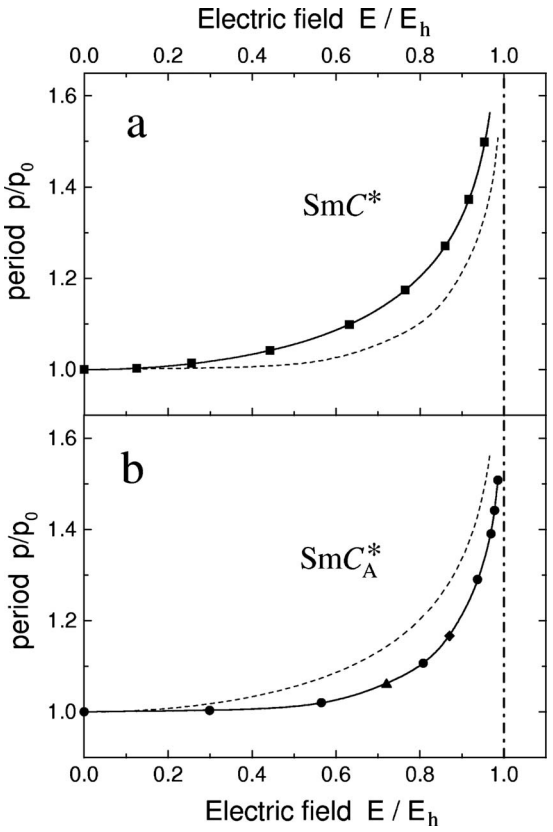

FIG. 2. Field dependence of the relative pitch p/p_0 for (a) ferroelectric and (b) antiferroelectric structures is shown by symbols. $p_0=79.6$ layers in the antiferroelectric phase (circles) and $p_0=159.2$ layers in the ferroelectric phase. The model parameters are $a=-1$, $f=1.975\times10^{-2}$ for the ferroelectric; $a=1$, $f=1.975\times10^{-2}$ for the antiferroelectric (circles); $a=0.75$, $f=1.975\times10^{-2}$ (triangle); $a=1$, $f=2.965\times10^{-2}$ (diamond). $E_hP_i\approx4.8\times10^{-4}$ in the ferroelectric phase and $E_hP_i\approx6.2\times10^{-2}$ in the antiferroelectric phase. The field dependence of p/p_0 differs in the Sm C^* and Sm C_A^* phases. For comparison, thin dashed lines are drawn in the figure. They correspond to the dependence of p/p_0 in the (a) antiferroelectric and (b) ferroelectric structures. The dashed curves and the solid curve for antiferroelectric are drawn to guide the eye.

and $a=1$ and $f=1.975\times10^{-2}$ in Sm C_A^* (circles), which correspond to $p_0\approx159.2$ layers in the ferroelectric phase and $p_0\approx79.6$ layers in the antiferroelectric phase. The triangle and diamond in Fig. 2(b) show the results of calculations correspondingly for $a=0.75$, $f=1.975\times10^{-2}$ and $a=1$, $f=2.965\times10^{-2}$. All points correspond to the same dependence, which represents the universal behavior of p/p_0 versus E/E_h. In electric field the helix becomes distorted. In this structure domains with smaller winding are separated by domain walls with a larger angle between nearest tilt planes. The distance between domain walls and hence the pitch increase with field. In the ferroelectric phase the numerical calculations give a value of $E_hP_i\approx4.8\times10^{-4}$ where the transition to the unwound state occurs. For the ferroelectric the equation describing the unwinding of the helix and the critical field E_h found in the continuum model [3–13] can be rewritten in terms of the discrete model. The interlayer synclinic interaction $\frac{1}{2}a(\xi_i\cdot\xi_{i+1})$ in Eq. (1) corresponds in the

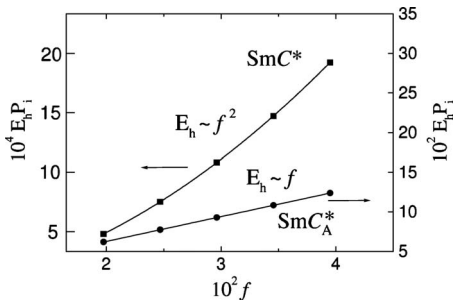

FIG. 3. Dependence of the critical field E_h on the value of chiral interaction f in antiferroelectric (circles) and ferroelectric (squares) phases. $a=1$ in the antiferroelectric phase and $a=-1$ in the ferroelectric phase. $f=1.975\times10^{-2}$ corresponds to zero-field pitch $p_0=79.6$ layers in the antiferroelectric phase and $p_0=159.2$ layers in the ferroelectric phase. The pitch decreases with increasing f. In the ferroelectric phase the solid curve is drawn according to Eq. (2). In the antiferroelectric phase the solid line is a fit of the data by a linear dependence.

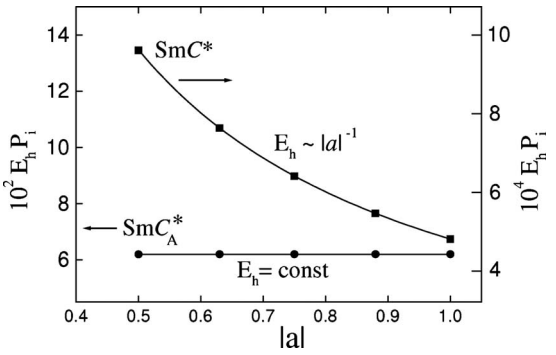

FIG. 4. Dependence of the critical field E_h on the value of anticlinic (a) and synclinic ($-a$) interlayer interaction in the antiferroelectric (circles) and the ferroelectric (squares) phases. $f=1.975\times10^{-2}$ in ferroelectric and antiferroelectric. $|a|=1$ corresponds to zero-field pitch $p_0=79.6$ layers in the antiferroelectric phase and $p_0=159.2$ layers in the ferroelectric phase. The pitch $p_0\sim|a|$, that is, decreases with decreasing $|a|$. In the ferroelectric phase the solid curve is drawn according to Eq. (2). In antiferroelectric the critical field does not depend on a (the solid line is $E_hP_i=6.2\times10^{-2}$).

continuous model to Frank energy $\frac{1}{2}K(\frac{\partial\varphi}{\partial z})^2$ [1], chiral interaction $f[\xi_i\times\xi_{i+1}]_z$—to a term $\Lambda(\frac{\partial\varphi}{\partial z})$, where K is the twist elastic constant and Λ is the Lifshitz parameter. Using the linkage between two models [31] the analytical equation for E_h is written as

$$E_h=\frac{\pi^2}{8}\frac{f^2}{|a|P_i}. \tag{2}$$

For the used model parameters $E_hP_i\approx4.81\times10^{-4}$, which well coincides with the results of numerical calculations (4.8×10^{-4}). The solid curve in Fig. 2(a) shows the variation of p/p_0 in the ferroelectric phase found from the continuous model. So, in ferroelectric liquid crystals the field variation of the pitch and the value of the critical field E_h calculated from the discrete and continuous models well agree.

In antiferroelectric the critical field E_h is essentially larger than in ferroelectric. Figures 3 and 4 show the dependence of E_hP_i on the model parameters. The results of numerical calculations are shown by squares (Sm C^*) and circles (Sm C_A^*). In ferroelectric, E_h changes in accordance with Eq. (2) (solid curve). The critical field E_h increases as the square of the value of the chiral interaction f (Fig. 3) and is inversely proportional to the synclinic interaction $|a|$ between layers (Fig. 4). An essentially different dependence was found in antiferroelectric. The critical electric field E_h is proportional to the value of the chiral interaction f (Fig. 3) and does not depend on the anticlinic interaction a between nearest layers (Fig. 4). To the best of our knowledge this behavior of the critical field in antiferroelectric liquid crystals was not known earlier. The linear dependence of E_h on f and its independence on $|a|$ were found with good accuracy for $|f/a|<4\times10^{-2}$. It is useful to know the dependence of E_h on measured values, for instance, on the helical pitch. For a long pitch ($p_0>30$) in the ferroelectric phase $p_0=-\pi a/f$, and in the antiferroelectric phase $p_0=\pi a/2f$. Usually the helical pitch in mixtures is increased or decreased by changing chirality (f in the discrete model). The critical field in ferroelectric $E_h=\pi^4|a|/8p_0^2P_i$ is proportional to p_0^{-2}. From Fig. 3 it follows that in antiferroelectric E_h is proportional to f, that is, $E_h\sim p_0^{-1}$.

The evolution of the pitch p with field differs in Sm C^* and Sm C_A^* (Fig. 2). In order to make the difference clear, we draw in Fig. 2 dashed curves which correspond to p/p_0 in the antiferroelectric phase [Fig. 2(a)] and in the ferroelectric phase [Fig. 2(b)]. The antiferroelectric pitch changes slightly at small electric field and increases drastically at high field [Fig. 2(b)]. This dependence of the pitch on field is related to the structure of the Sm C_A^* phase and its specific transformation in electric field. In ferroelectric in low electric field the net local polarization P_F^L is about nP_i, where $n\ll p_0$ is the number of layers ($P_F^L\approx2P_i$ for a synclinic pair). In antiferroelectric the net polarization of an anticlinic pair $P_A^L=2P_i\sin\alpha/2\approx P_i\alpha$ is essentially smaller than in ferroelectric ($P_i\alpha\ll2P_i$). This leads to a small change in the antiferroelectric pitch in low field. Reorientation of the molecules in electric field decreases the local electrostatic energy F_E. In ferroelectric F_E decreases due to rotation of P_F^L toward the direction of the field. In antiferroelectric F_E decreases due to reorientation of P_A^L and increase in α and P_A^L, which becomes essential in high field. This leads to a sharper dependence of the pitch on the electric field with respect to ferroelectric close to the critical field [Fig. 2(b)]. After the transition to the unwound state polarization of all anticlinic pairs becomes parallel to the electric field [19,32].

The independence of E_h on the anticlinic interlayer interaction a may be explained in the following manner: with increasing a the pitch p_0 increases, but the angle between nearest tilt planes also increases, i.e., the polarization of the anticlinic pairs decreases. The increase in p_0 and decrease in the polarization of the anticlinic pairs lead to independence of E_h on a. The same situation will take place in ferroelectric (where $E_h=\pi^3f/8p_0P_i$) if we increase p_0 and proportionally decrease P_i. In antiferroelectric the increase in a automatically increases p_0 and decreases the effective polarization of anticlinic pairs. This qualitatively explains the independence of E_h on a.

We remind that the pitch p/p_0 in the Sm C_A^* phase changes slightly in small field and increases drastically at high field. This dependence may resemble a threshold behavior especially in cells with the Fréedericksz transition [17,18], when surface anchoring plays a substantial role. In our calculations of the Sm C_A^* phase for fields $E/E_h < 0.3$ we cannot argue whether the helix unwinding is characterized by a threshold or not. In materials with intermediate subphases [33,34], field-induced antiferroelectric-ferrielectric-ferroelectric transitions can occur. We do not investigate subphases in our paper since this is a special topic which will be studied in another work.

It should be noted that model parameters in Eq. (1) depend on the tilt angle θ. In the discrete phenomenological model interlayer interactions in Eq. (1) vary with the square of θ [25–31]; layer polarization P_i increases with θ. So in ferroelectric and antiferroelectric materials we may assume a similar dependence of the critical field on θ. For instance, in materials with $P_i \sim \theta$ the critical field $E_h \sim \theta$. When data are compared at different temperatures these dependencies on θ should be taken into account.

In various systems with two or more competing periodicities, sequences of structures known as the "devil's staircase" and the "harmless staircase" can appear [35–37]. Periods of different structures in these sequences scale as rational numbers. Such a sequence of structures has been proposed as the first model of intermediate subphases in polar liquid crystals [14] and is expected to appear in the short-pitch smectic-C_α^* phase in external field [31]. This behavior should be most pronounced in ultrashort-pitch structures when the zero-field period is on the order of several molecular layers. With increasing the helical pitch the field-induced evolution of structures should approach to the one given by the continuous model and can be effectively represented by a smooth curve [31]. In our calculations the zero-field pitch is essentially larger than the layer spacing.

Now we estimate the critical field E_h in antiferroelectric from the free energy (1). We use a similar procedure to that used by Kamien and Selinger [2] for ferroelectric. The free energy of the uniform twisted state is $F_t = -N(1/2a \cos\alpha + f \sin\alpha)$, where $\alpha \approx 2f/a$ and N is the number of layers in the sample. The free energy of the unwound state is $F_u = -N(1/2a \cos\alpha_1 + EP_i \sin\alpha_1/2)$, where α_1 is the angle after unwinding of the helix. The critical field E_h can be evaluated by taking $\alpha = \alpha_1$ and F_t equal to F_u. For small α our estimation gives $E_h = 2f/P_i$. This equation gives a right dependence of the critical field on f (Fig. 3) and its independence on a (Fig. 4). However, the value of the critical field found from the equation $E_h = 2f/P_i$ is smaller than E_h obtained in our calculations. It is not a surprising result since in the estimation of E_h we neglected the transformation of the helix in electric field, i.e., we considered $\alpha = \text{const}$. The actual unwinding field is larger since the structure with the deformed helix can adjust to the field and thus exist at a larger field than $2f/P_i$. The coefficient at f/P_i can be obtained from the numerical calculations of the dependence of the critical field E_h on the ratio f/P_i. It gives

$$E_h = 3.14\frac{f}{P_i}. \tag{3}$$

The obtained coefficient is very close to π. We may guess that it is not an accident and an exact equation exists for the critical field of antiferroelectric in the form of $E_h = \pi f/P_i$.

In summary, the unwinding of the antiferroelectric helical structure in electric field was studied using the discrete phenomenological model. The field dependence of the helical pitch and the critical field E_h at which the helical structure transforms into the unwound structure were calculated. We found that the dependence of the critical field E_h on the interlayer nonchiral (a) and chiral (f) interactions differs essentially in antiferroelectric and ferroelectric phases. In the antiferroelectric phase the critical electric field E_h is proportional to the value of chiral interaction and does not depend on the anticlinic interaction between nearest layers, namely, on the twist elastic constant. Based on our calculations, an analytical equation is proposed for the critical unwinding field of the antiferroelectric helix.

ACKNOWLEDGMENT

This work was supported in part by the RFFI under Grant No. 08-02-00827.

[1] P. G. de Gennes and J. Prost, *The Physics of Liquid Crystals*, 2nd ed. (Clarendon, Oxford, 1993).
[2] R. D. Kamien and J. V. Selinger, J. Phys.: Condens. Matter **13**, R1 (2001).
[3] P. G. de Gennes, Solid State Commun. **6**, 163 (1968).
[4] R. B. Meyer, Appl. Phys. Lett. **12**, 281 (1968).
[5] R. B. Meyer, Appl. Phys. Lett. **14**, 208 (1969).
[6] A. Michelson, L. Benguigui, and D. Cabib, Phys. Rev. A **16**, 394 (1977).
[7] H. Takezoe, K. Furuhata, T. Nakagiri, A. Fukuda, and E. Kure, Jpn. J. Appl. Phys. **17**, 1219 (1978).
[8] S. A. Pikin and V. L. Indenbom, Sov. Phys. Usp. **21**, 487 (1978) [Usp. Fiz. Nauk **125**, 251 (1978)].
[9] V. E. Dmitrienko and V. A. Belyakov, Zh. Eksp. Teor. Fiz. **78**, 1568 (1980) [JETP **51**, 787 (1980)].
[10] B. Kutnjak-Urbanc and B. Žekš, Phys. Rev. E **51**, 1569 (1995).
[11] N. Baytch, R. L. B. Selinger, J. V. Selinger, and R. Shashidhar, Phys. Rev. E **68**, 041702 (2003).
[12] F. Ghoddoussi, M. A. Pantea, P. H. Keyes, R. Naik, and P. P. Vaishnava, Phys. Rev. E **68**, 051706 (2003).
[13] Z. Kutnjak, Phys. Rev. E **70**, 061704 (2004).
[14] A. Fukuda, Y. Takanishi, T. Isosaki, K. Ishikawa, and H. Takezoe, J. Mater. Chem. **4**, 997 (1994).
[15] I. Muševič, B. Žekš, R. Blinc, and Th. Rasing, Phys. Rev. E **47**, 1094 (1993).
[16] X. Y. Wang and P. L. Taylor, Phys. Rev. Lett. **76**, 640 (1996).
[17] X. Y. Wang, T. Kyu, A. M. Rudin, and P. L. Taylor, Phys. Rev.

E **58**, 5919 (1998).
[18] T. Qian and P. L. Taylor, Phys. Rev. E **60**, 2978 (1999).
[19] J. P. F. Lagerwall, Phys. Rev. E **71**, 051703 (2005).
[20] H. Orihara, Y. Naruse, M. Yagyu, A. Fajar, and S. Uto, Phys. Rev. E **72**, 040701(R) (2005).
[21] P. V. Dolganov and V. M. Zhilin, Phys. Rev. E **77**, 031703 (2008).
[22] P. V. Dolganov, V. M. Zhilin, V. K. Dolganov, and E. I. Kats, Pis'ma Zh. Eksp. Teor. Fiz. **89**, 181 (2009) [JETP Lett. **89**, 161 (2009)].
[23] A. V. Emelyanenko, Eur. Phys. J. E **28**, 441 (2009).
[24] H. Sun, H. Orihara, and Y. Ishibashi, J. Phys. Soc. Jpn. **62**, 2706 (1993).
[25] M. Čepič and B. Žekš, Mol. Cryst. Liq. Cryst. Sci. Technol., Sect. A **263**, 61 (1995).
[26] A. Roy and N. V. Madhusudana, EPL **41**, 501 (1998).
[27] B. Rovšek, M. Čepič, and B. Žekš, Phys. Rev. E **62**, 3758 (2000).
[28] L. A. Parry-Jones and S. J. Elston, Phys. Rev. E **63**, 050701(R) (2001).
[29] D. A. Olson, X. F. Han, A. Cady, and C. C. Huang, Phys. Rev. E **66**, 021702 (2002).
[30] P. V. Dolganov, V. M. Zhilin, V. K. Dolganov, and E. I. Kats, Phys. Rev. E **67**, 041716 (2003).
[31] B. Rovšek, M. Čepič, and B. Žekš, Phys. Rev. E **70**, 041706 (2004).
[32] J.-K. Song, Atsuo Fukuda, and J. K. Vij, Phys. Rev. E **76**, 011708 (2007).
[33] E. Gorecka, A. D. L. Chandani, Y. Ouchi, H. Takezoe, and A. Fukuda, Jpn. J. Appl. Phys., Part 1 **29**, 131 (1990).
[34] K. Hiraoka, E. Gorecka, A. D. L. Chandani, Y. Ouchi, H. Takezoe, and A. Fukuda, Jpn. J. Appl. Phys., Part 2 **29**, L1473 (1990).
[35] S. Aubry, Lect. Notes Math. **925**, 221 (1982).
[36] S. Aubry, J. P. Gosso, G. Abramovici, J. L. Raimbault, and P. Quemerais, Physica D **47**, 461 (1991).
[37] P. M. Chaikin and T. C. Lubensky, *Principles of Condensed Matter Physics* (Cambridge University Press, Cambridge, England, 1995).